

## Tuning Peptoid Secondary Structure with Pentafluoroaromatic Functionality: A New Design Paradigm for the Construction of Discretely Folded Peptoid Structures

Benjamin C. Gorske and Helen E. Blackwell\*

Contribution from the Department of Chemistry, University of Wisconsin—Madison,  
1101 University Avenue, Madison, Wisconsin 53706-1322

Received July 21, 2006; E-mail: blackwell@chem.wisc.edu

**Abstract:** Peptoids, or oligomers of *N*-substituted glycine, are an important class of non-native polymers whose close structural similarity to natural  $\alpha$ -peptides and ease of synthesis offer significant advantages for the study of biomolecular interactions and the development of biomimetics. Peptoids that are *N*-substituted with  $\alpha$ -chiral aromatic side chains have been shown to adopt either helical or “threaded loop” conformations, depending upon solvent and oligomer length. Elucidation of the factors that impact peptoid conformation is essential for the development of general rules for the design of peptoids with discrete and novel structures. Here, we report the first study of the effects of pentafluoroaromatic functionality on the conformational profiles of peptoids. This work was enabled by the synthesis of a new,  $\alpha$ -chiral amine building block, (*S*)-1-(pentafluorophenyl)ethylamine (*S*-2), which was found to be highly compatible with peptoid synthesis (delivering (*S*)-*N*-(1-(pentafluorophenyl)ethyl)glycine oligomers). The incorporation of this fluorinated monomer unit allowed us to probe both the potential for  $\pi$ -stacking interactions along the faces of peptoid helices and the role of side chain electrostatics in peptoid folding. A series of homo- and heteropeptoids derived from *S*-2 and non-fluorinated,  $\alpha$ -chiral aromatic amide side chains were synthesized and characterized by circular dichroism (CD) and nuclear magnetic resonance (NMR) spectroscopy. Enhancement of  $\pi$ -stacking by quadrupolar interactions did not appear to play a significant role in stabilizing the conformations of heteropeptoids with alternating fluorinated and non-fluorinated side chains. However, incorporation of (*S*)-*N*-(1-(pentafluorophenyl)ethyl)glycine monomers enforced helicity in peptoids that typically exhibit threaded loop conformations. Moreover, we found that the incorporation of a single (*S*)-*N*-(1-(pentafluorophenyl)ethyl)glycine monomer could be used to selectively promote looped or helical structure in this important peptoid class by tuning the electronics of nearby heteroatoms. The strategic installation of this monomer unit represents a new approach for the manipulation of canonical peptoid structure and the construction of novel peptoid architectures.

### Introduction

Peptoids, or oligomers of *N*-substituted glycine, have emerged as a versatile class of peptidomimetics for the study of biomolecular interactions.<sup>1,2</sup> Interest in peptoids as tools for chemical biology and biotechnology continues to increase due to the relative ease with which they can be synthesized,<sup>3,4</sup> their resistance to proteolytic degradation,<sup>5</sup> and the wide variety of non-native functionality that can be incorporated. These advantages have motivated the development of peptoids for a broad range of applications, including antimicrobial agents,<sup>6</sup> lung

surfactants,<sup>7</sup> high-density ligand arrays,<sup>8</sup> activation domain mimics,<sup>9</sup> inhibitors of protein–protein interactions,<sup>10</sup> and vehicles for gene and drug delivery.<sup>11</sup> In turn, this work has prompted an examination of the role of secondary structure in peptoid function.<sup>12</sup> However, as with peptides and proteins, the design and prediction of peptoid structure *a priori* presents a

- (1) Simon, R. J.; Kania, R. S.; Zuckermann, R. N.; Huebner, V. D.; Jewell, D. A.; Banville, S.; Ng, S.; Wang, L.; Rosenberg, S.; Marlowe, C. K.; Spellmeyer, D. C.; Tan, R.; Frankel, A. D.; Santi, D. V.; Cohen, F. E.; Bartlett, P. A. *Proc. Natl. Acad. Sci. U.S.A.* **1992**, *89*, 9367–9371.
- (2) For reviews of peptoids, see: (a) Patch, J. A.; Kirshenbaum, K.; Seuryneck, S. L.; Zuckermann, R. N.; Barron, A. E. In *Pseudopeptides in Drug Development*; Nielsen, P. E., Ed.; Wiley-VCH: Weinheim, Germany, 2004. (b) Patch, J. A.; Barron, A. E. *Curr. Opin. Chem. Biol.* **2002**, *6*, 872–877.
- (3) Zuckermann, R. N.; Kerr, J. M.; Kent, S. B. H.; Moos, W. H. *J. Am. Chem. Soc.* **1992**, *114*, 10646–10647.
- (4) Alluri, P. G.; Reddy, M. M.; Bachhawat-Sikder, K.; Olivos, H. J.; Kodadek, T. *J. Am. Chem. Soc.* **2003**, *125*, 13995–14004.
- (5) Miller, S. M.; Simon, R. J.; Ng, S.; Zuckermann, R. N.; Kerr, J. M.; Moos, W. H. *Bioorg. Med. Chem. Lett.* **1994**, *4*, 2657–2662.

- (6) Patch, J. A.; Barron, A. E. *J. Am. Chem. Soc.* **2003**, *125*, 12092–12093.
- (7) Seuryneck, S. L.; Patch, J. A.; Barron, A. E. *Chem. Biol.* **2005**, *12*, 77–88.
- (8) Li, S.; Bowerman, D.; Marthandan, N.; Klyza, S.; Luebke, K. J.; Garner, H. R.; Kodadek, T. *J. Am. Chem. Soc.* **2004**, *126*, 4088–4089.
- (9) Liu, B.; Alluri, P. G.; Yu, P.; Kodadek, T. *J. Am. Chem. Soc.* **2005**, *127*, 8254–8255.
- (10) Hara, T.; Durell, S. R.; Myers, M. C.; Appella, D. H. *J. Am. Chem. Soc.* **2006**, *128*, 1995–2004.
- (11) Wender, P. A.; Mitchell, D. J.; Pattabiraman, K.; Pelkey, E. T.; Steinman, L.; Rothbard, J. B. *Proc. Natl. Acad. Sci. U.S.A.* **2000**, *97*, 13003–13008.
- (12) (a) Kirshenbaum, K.; Barron, A. E.; Goldsmith, R. A.; Armand, P.; Bradley, E. K.; Truong, K. T.; Dill, K. A.; Cohen, F. E.; Zuckermann, R. N. *Proc. Natl. Acad. Sci. U.S.A.* **1998**, *95*, 4303–4308. (b) Wu, C. W.; Sanborn, T. J.; Zuckermann, R. N.; Barron, A. E. *J. Am. Chem. Soc.* **2001**, *123*, 2958–2963. (c) Wu, C. W.; Sanborn, T. J.; Huang, K.; Zuckermann, R. N.; Barron, A. E. *J. Am. Chem. Soc.* **2001**, *123*, 6778–6784. (d) Wu, C. W.; Kirshenbaum, K.; Sanborn, T. J.; Patch, J. A.; Huang, K.; Dill, K. A.; Zuckermann, R. N.; Barron, A. E. *J. Am. Chem. Soc.* **2003**, *125*, 13525–13530. (e) Huang, K.; Wu, C. W.; Sanborn, T. J.; Patch, J. A.; Kirshenbaum, K.; Zuckermann, R. N.; Barron, A. E.; Radhakrishnan, I. *J. Am. Chem. Soc.* **2006**, *128*, 1733–1738.

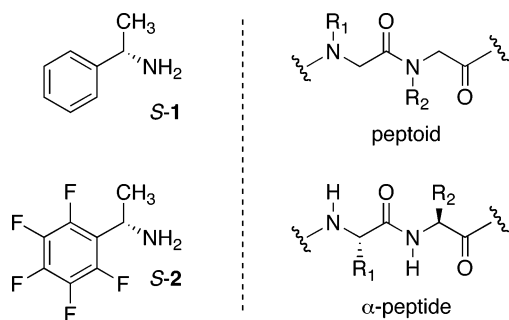


**Figure 1.** (Left)  $\alpha$ -Chiral aromatic amine building blocks **S-1** and **S-2**. (Right) A comparison of peptoids and  $\alpha$ -peptides.

formidable challenge. At the root of this challenge lies the need to further develop our understanding of noncovalent interactions and how they affect the folding of both natural and synthetic polymers.<sup>13</sup> Hydrophobic,<sup>14</sup> ionic,<sup>15</sup> hydrogen bonding,<sup>16</sup> and aromatic interactions<sup>17</sup> are among the many noncovalent interactions implicated in ordering the structures of folded molecules. We sought to examine these interactions within a peptoid framework as part of an effort to develop new design strategies for generating well-folded peptoids.<sup>18</sup> Our initial investigations have focused on the role of aromatic interactions in this context, since these are believed to significantly influence the folding of not only peptoids (*vide infra*), but also a wide range of natural and non-natural foldamers.<sup>17,19</sup>

Pioneering research by Barron, Zuckermann, Dill, and co-workers revealed the first design strategy for the generation of stable secondary structures in peptoids. In this past work, the incorporation of certain  $\alpha$ -chiral aromatic and aliphatic amide side chains was found to enforce stable helical structure in peptoids similar to that of the polyproline type I helix in  $\alpha$ -peptides.<sup>12</sup> The majority of these studies have focused on peptoids composed predominately of either (*R*)- or (*S*)-*N*-(1-phenylethyl)glycine (designated *Nrpe* or *Nspe*, respectively), which are constructed from commercially available (*R*)- or (*S*)-1-phenylethylamine building blocks (**S-1**, Figure 1) using the well-established, submonomer peptoid synthesis method.<sup>3</sup> The peptoid helix consists entirely of *cis*-amide bonds and has a periodicity of ca. three residues per turn and a pitch of ca. 6 Å; helix sense is determined by the handedness of the  $\alpha$ -chiral side chains, with *S*- and *R*-side chains giving right- and left-handed peptoid helices, respectively.<sup>12</sup> Helix formation is particularly promoted in these systems by the incorporation of aromatic side chains with 3-fold periodicity, which creates “aromatic faces” along the length of the peptoid helix.<sup>12c</sup> Attractive, intramo-

lecular  $\pi$ -stacking interactions along these faces have been proposed to play a role in stabilizing peptoid helices.<sup>20,21</sup> Alternatively, intermolecular side chain interdigitation has also been examined as a mechanism for helix stabilization.<sup>12b</sup> These aromatic interactions, in conjunction with steric and stereoelectronic repulsions between the side chains and the backbone, are presumed to be critical for folding, as the peptoid backbone is devoid of features known to otherwise dictate peptide and protein folding, i.e., hydrogen-bond donors and main chain chirality (Figure 1).

The potential significance of aromatic–aromatic interactions in peptoid structures prompted our investigation of perfluorinated aromatic groups as components of peptoid side chains, as they possess nearly equal, but opposite, quadrupole polarities compared to non-fluorinated aryl rings.<sup>22</sup> Numerous studies suggest that favorable quadrupolar interactions between properly aligned aromatic and perfluoroaromatic rings can enhance  $\pi$ -stacking interactions.<sup>21,23</sup> However, recent explorations of this phenomenon using a peptide  $\alpha$ -helix scaffold did not provide evidence for aromatic–perfluoroaromatic attractions stronger than those of the aryl–aryl type.<sup>24</sup> The authors of this previous study proposed that incorrect alignment and spacing of the aromatic rings were likely responsible for the lack of additional stabilization. As peptoids have substantially higher conformational flexibility relative to peptides,<sup>1,2</sup> we reasoned that peptoids would provide an improved scaffold for the further exploration of aromatic–perfluoroaromatic interactions in foldamers. Indeed, this flexibility would be essential for the observation of face-to-face intramolecular aromatic interactions, as these typically require interplanar distances on the order of 3.5 Å<sup>25</sup>—far less than those observed between side chains in the solid-state and NMR structures of peptoid helices (ca. 6 Å).<sup>12d,20a</sup> We hypothesized that these interactions, if operative in peptoids, could be exploited to enhance peptoid helix stability. Furthermore, perturbation of the side chain electronics and steric contours by fluorination could illuminate other factors relevant to peptoid folding, such as hydrophobic or inductive effects.

In this work, we report the synthesis of (*S*)-1-(pentafluorophenyl)ethan-1-amine (**S-2**) and the incorporation of this new, chiral, perfluoroaromatic building block into a series of peptoids. This synthetic work has enabled the first evaluation of the effects of pentafluoroaromatic side chain functionality on the conformational profiles of peptoids. These studies have revealed that pentafluoroaromatic side chains can stabilize peptoid secondary structures via a mechanism that is distinct from the quadrupole-enhanced  $\pi$ -stacking mechanism that we had originally proposed. Namely, this new peptoid synthon enables site-selective tuning of hydrogen bonds to peptoid backbone heteroatoms,

- (13) (a) Gellman, S. H. *Acc. Chem. Res.* **1998**, *31*, 173–180. (b) Hill, D. J.; Mio, M. J.; Prince, R. B.; Hughes, T. S.; Moore, J. S. *Chem. Rev.* **2001**, *101*, 3893–4012.
- (14) Southall, N. T.; Dill, K. A.; Haymet, A. D. J. *J. Phys. Chem. B* **2002**, *106*, 521–533.
- (15) Kumar, S.; Nussinov, R. *ChemBioChem* **2002**, *3*, 604–617.
- (16) (a) Dill, K. A. *Biochemistry* **1990**, *29*, 7133–7155. (b) Appella, D. H.; Christianson, L. A.; Karle, I. L.; Powell, D. R.; Gellman, S. H. *J. Am. Chem. Soc.* **1996**, *118*, 13071–13072. (c) Meot-Ner, M. *Chem. Rev.* **2005**, *105*, 213–284.
- (17) (a) Waters, M. L. *Biopolymers* **2004**, *76*, 435–445. (b) Waters, M. L. *Curr. Opin. Chem. Biol.* **2002**, *6*, 736–741.
- (18) Gorske, B. C.; Jewell, S. A.; Guerard, E. J.; Blackwell, H. E. *Org. Lett.* **2005**, *7*, 1521–1524.
- (19) For selected examples, see: (a) Graciani, N. R.; Tsang, K. Y.; McCutchen, S. L.; Kelly, J. W. *Bioorg. Med. Chem.* **1994**, *2*, 999–1006. (b) Prince, R. B.; Saven, J. G.; Wolyynes, P. G.; Moore, J. S. *J. Am. Chem. Soc.* **1999**, *121*, 3114–3121. (c) Gabriel, G. J.; Sorey, S.; Iverson, B. L. *J. Am. Chem. Soc.* **2005**, *127*, 2637–2640. (d) Mahalakshmi, R.; Raghothama, S.; Balaram, P. *J. Am. Chem. Soc.* **2006**, *128*, 1125–1138. (e) Hu, Z.-Q.; Hu, H.-Y.; Chen, C.-F. *J. Org. Chem.* **2006**, *71*, 1131–1138.

- (20) (a) Armand, P.; Kirshenbaum, K.; Goldsmith, R. A.; Farr-Jones, S.; Barron, A. E.; Truong, K. T.; Dill, K. A.; Mierke, D. F.; Cohen, F. E.; Zuckermann, R. N.; Bradley, E. K. *Proc. Natl. Acad. Sci. U.S.A.* **1998**, *95*, 4309–4314. (b) Armand, P.; Kirshenbaum, K.; Falicov, A.; Dunbrack, R. L. Jr.; Dill, K. A.; Zuckermann, R. N.; Cohen, F. E. *Folding Des.* **1997**, *2*, 369–375.
- (21) For an excellent review of aromatic–aromatic interactions, see: Meyer, E. A.; Castellano, R. K.; Diederich, F. *Angew. Chem., Int. Ed.* **2003**, *42*, 1210–1250.
- (22) Battaglia, M. R.; Buckingham, A. D.; Williams, J. H. *Chem. Phys. Lett.* **1981**, *78*, 420–423.
- (23) Coates, G. W.; Dunn, A. R.; Henling, L. M.; Dougherty, D. A.; Grubbs, R. H. *Angew. Chem., Int. Ed. Engl.* **1997**, *36*, 248–251.
- (24) Butterfield, S. M.; Patel, P. R.; Waters, M. L. *J. Am. Chem. Soc.* **2002**, *124*, 9751–9755.
- (25) (a) Patrick, C. R.; Prosser, G. S. *Nature (London)* **1960**, *187*, 1021. (b) Williams, V. E.; Lemieux, R. P.; Thatcher, G. R. J. *J. Org. Chem.* **1996**, *61*, 1927–1933. (c) Xu, R.; Gramlich, V.; Frauenrath, H. *J. Am. Chem. Soc.* **2006**, *128*, 5541–5547.

while simultaneously preserving a steric profile that supports helix formation. Here, we demonstrate exquisite control over peptoid nonamer folding by the strategic incorporation of a single (*S*)-*N*-(1-(pentafluorophenyl)ethyl)glycine, or “*N*sf”, monomer unit. This new design principle has facilitated the construction of well-folded peptoids with unprecedented stability and should significantly expand the potential of peptoids as chemical tools in numerous applications. Furthermore, when installed in conjunction with hydrogen bonding side chains, this pentafluoroaromatic monomer could provide access to heretofore unknown peptoid structures that are stabilized by additional, tunable hydrogen bonds.

## Experimental Section

**General.** All reagents were purchased from commercial sources (Alfa-Aesar, Aldrich, Advanced ChemTech, and Acros) and used without further purification. Solvents were purchased from commercial sources (Aldrich and J. T. Baker) and used as is, with the exception of dichloromethane (CH<sub>2</sub>Cl<sub>2</sub>), which was distilled over calcium hydride immediately prior to use. Fmoc-protected, Rink amide linker-derivatized polystyrene resin (100–200 mesh, loading = 0.69 mmol/g; Advanced ChemTech) was used for all solid-phase syntheses. Full details of the instrumentation and analytical methods used in this work can be found in the Supporting Information.

**Synthesis of (*S*)-1-(Pentafluorophenyl)ethyl Azide (*S*-4).** Diphenylphosphoryl azide (DPPA, 1.12 mL, 5.19 mmol) and diethyl azodicarboxylate (DEAD, 1.00 mL, 5.19 mmol) were cannulated into a dry 50 mL flask containing 25 mL of dry tetrahydrofuran (THF) and immersed in an ice–water bath. The solution was stirred under N<sub>2</sub> for 15 min, after which a solution of (*R*)-(+)-1-(pentafluorophenyl)ethanol (1.00 g, 4.72 mmol) in dry THF was cannulated into the flask. The solution was stirred under N<sub>2</sub> for an additional 15 min while immersed in the ice–water bath. Triphenylphosphine (PPh<sub>3</sub>, 1.11 g, 4.25 mmol) was dissolved in dry THF and cannulated into the flask. The reaction was stirred for 15 min under N<sub>2</sub>, after which it was sealed and placed in a freezer at –5 °C for 16 h. The THF was subsequently removed by careful distillation to give a yellow, viscous residue that was further purified by flash silica gel column chromatography (pentane). The pentane was removed by careful distillation to afford 1.84 g of a clear liquid that was 47% (*S*)-1-(pentafluorophenyl)ethyl azide (*S*-4) by mass, as indicated by <sup>1</sup>H NMR (remaining mass was residual pentane).<sup>26</sup> 77% yield. TLC *R*<sub>f</sub> = 0.36 (pentane); <sup>1</sup>H NMR (CDCl<sub>3</sub>, 300 MHz) δ 5.01 (q, *J* = 7.1 Hz, 1H), 1.67 (d, *J* = 7.1 Hz, 3H); <sup>13</sup>C NMR (CDCl<sub>3</sub>, <sup>1</sup>H broadband-decoupled, 75 MHz) δ 145.0 (dddd, *J*<sub>CF</sub> = 249.8, 17.0, 8.3, 4.6 Hz), 141.1 (dt, *J*<sub>CF</sub> = 256.7, 13.6, 5.3 Hz), 137.7 (dddd, *J*<sub>CF</sub> = 252.8, 16.5, 12.7, 4.9, 2.3 Hz); <sup>19</sup>F NMR (CDCl<sub>3</sub>) δ –142.4 (dd, *J* = 21.5, 5.8 Hz, 2F), –153.7 (t, *J* = 21.5 Hz, 1F), –161.1 (ddd, *J* = 21.5, 21.5, 6.5 Hz, 2F); IR (ATR): 3342, 2992, 2944, 2115, 1653, 1503, 1459, 1425, 1358, 1305, 1244, 1152, 1026, 971, 917, 848 cm<sup>–1</sup>; EI-MS: expected *m/z* 237.0, observed *m/z* 237.0 [M]<sup>+</sup>; [β]<sub>D</sub><sup>25</sup> = +7.28° (CDCl<sub>3</sub>, *c* = 0.055).

**Synthesis of (*S*)-1-(Pentafluorophenyl)ethylamine (*S*-2).**<sup>27</sup> Azide *S*-4 (196.3 mg, 0.83 mmol) was dissolved in 10 mL of THF in a dry 25 mL flask. PPh<sub>3</sub> (435.0 mg, 1.66 mmol) was dissolved in 15 mL of THF and added dropwise to the stirred solution. After the bubbling of N<sub>2</sub> had subsided, distilled H<sub>2</sub>O (134 mL, 7.45 mmol) was added, and the reaction mixture was stirred for 16 h at 45 °C. The solvent was removed *in vacuo*, and the product was purified by flash silica gel chromatography (1:1 pentane/ethyl acetate (EtOAc) with 1% triethyl-

amine). The eluent was removed by careful distillation to afford 162.2 mg of a yellow liquid that was 68% amine *S*-2 by mass, as indicated by <sup>1</sup>H NMR analysis (remaining mass was residual pentane/EtOAc).<sup>26</sup> 49% yield overall. An ee of >99% was determined by reversed-phase high performance liquid chromatography (RP-HPLC) using a Daicel Chemical Industries Chiralcel OD-H column (flow rate = 1 mL/min, 1% ethanol/hexanes; UV detection at 260 nm; retention time = 20.9 min).<sup>28</sup> TLC *R*<sub>f</sub> = 0.25 (1:1 pentane/EtOAc with 1% triethylamine); <sup>1</sup>H NMR (CDCl<sub>3</sub>, 300 MHz) δ 4.47 (q, *J* = 7.0 Hz, 1H), 1.54 (dt, *J* = 7.0, 0.9 Hz, 3H); <sup>13</sup>C NMR (CDCl<sub>3</sub>, <sup>1</sup>H broadband-decoupled, 75 MHz) δ 144.6 (multiplet), 139.9 (multiplet), 137.5 (multiplet), 120.3 (multiplet), 43.1 (s), 23.4 (s); <sup>19</sup>F NMR (CDCl<sub>3</sub>) δ –145.1 (dd, *J* = 23, 8 Hz, 2F), –157.1 (t, *J* = 21 Hz, 1F), –162.2 (ddd, *J* = 23, 23, 8 Hz, 2F); IR (ATR): 3394 (broad), 2984, 2938, 1738, 1652, 1521, 1500, 1460, 1376, 1300, 1245, 1132, 1115, 971, 939, 849 cm<sup>–1</sup>; EI-MS: expected *m/z* 211.0, observed *m/z* 212.1 [M + H]<sup>+</sup>; [β]<sub>D</sub><sup>25</sup> = –12.2° (CDCl<sub>3</sub>, *c* = 0.017).

**Peptoid Synthesis, Purification, and Characterization.** Peptoids **5–20** were synthesized according to the microwave-assisted synthesis procedure we reported previously (Table 1).<sup>18</sup> Amine building blocks (*S*)-1-phenylethylamine (*S*-1) and (*S*)-1-(pentafluorophenyl)ethylamine (*S*-2) were used for peptoid synthesis and were either purchased from Aldrich or synthesized as described above, respectively.<sup>29</sup> After acid-mediated cleavage from the resin, peptoid samples were analyzed by RP-HPLC (with UV detection) using a Restek Premier C18 column (5 μm, 4.6 mm × 25 cm). Initial purities were determined by integration at 220 nm and ranged from 42 to 84%. Peptoid oligomers **5–20** were purified to homogeneity (>97%) by preparative RP-HPLC using a Vydac protein and peptide C18 column (10 μm, 22 mm × 250 mm). The purified peptoids were lyophilized to afford white powders. The purities and molar masses of the purified peptoids were verified by analytical RP-HPLC and mass spectrometry, respectively (Table 1).

**Circular Dichroism Analyses.** Circular dichroism (CD) spectra were obtained on a Jasco J-715 spectropolarimeter with J-700 for Windows Standard Analysis software (v. 1.50.01). CD data were analyzed and plotted using Microsoft Excel 2004 and KaleidaGraph 4.0 software. Peptoid stock solutions were prepared by dissolving at least 2 mg of each peptoid in a precisely measured amount of spectroscopic grade acetonitrile (ca. 830 mg). The stock solutions then were diluted with spectroscopic grade acetonitrile to the desired concentration (ca. 60 μM) by mass using a Mettler-Toledo XS105 high-precision balance. CD spectra were obtained in a square quartz cell (path length 0.2 cm) at room temperature using a scan rate of 100 nm/min, with 20 averaged scans per spectrum. The spectrum of an acetonitrile blank was subtracted from the CD traces, and the resulting data were smoothed using the weighting function in KaleidaGraph 4.0.

**Heteronuclear Single Quantum Coherence (HSQC) NMR Analyses.** HSQC NMR experiments<sup>30</sup> were performed on a Varian Inova 600 MHz spectrometer using a 5 mm hpx probe. The data were processed using the Varian VNMR software package (v. 6.1C) and visualized using SPARKY software.<sup>31</sup> Peptoids **5**, **7**, and **9** were dissolved in acetonitrile-*d*<sub>3</sub> to give ca. 6 mM solutions. For analysis, 400 μL aliquots of these solutions were placed in a 5 mm Shigemi NMR tube that was susceptibility-matched for dimethyl sulfoxide. The HSQC experiments were performed at 24 °C using the following parameter values: spectral widths were 6794.6 Hz in the <sup>1</sup>H dimension and 27903.7 Hz in the <sup>13</sup>C dimension. The number of transients (nt) and number of increments (ni) were 24 and 512, respectively. The

(26) Amine *S*-2 and azide *S*-4 were unusually volatile when dissolved in organic solvents. Careful distillation ameliorated this effect, but nevertheless, the complete removal of solvents significantly reduced yields.

(27) Amine *S*-2 has been synthesized in racemic form previously using a different, and lower yielding, method. See: Petrova, T. D.; Savchenko, T. I.; Ardyukova, T. F.; Yakobson, G. G. *Izv. Sib. Otd. Akad. Nauk SSSR, Ser. Khim. Nauk* **1970**, *3*, 119–122.

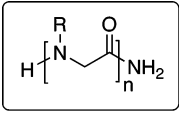
(28) Enantiomeric excess (99% ee) was determined by comparison of peak area percentages with those of a sample of racemic amine **2**.

(29) A 1.0 M solution of (*S*)-1-(pentafluorophenyl)ethylamine (*S*-2) in DMF was used for peptoid synthesis and was reused in coupling reactions up to 10 times without seriously compromising yields. This procedural modification allowed us to conserve this amine reagent.

(30) Boyer, R. D.; Johnson, R.; Krishnamurthy, K. J. *Magn. Reson.* **2003**, *165*, 253–259.

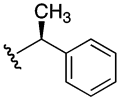
(31) Goddard, T. D.; Kneller, D. G. *SPARKY*, version 3.110; University of California: San Francisco, CA.

**Table 1.** Structures and Mass Spectrometry Data for Peptoid Oligomers 5–20<sup>a</sup>

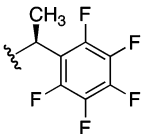


*N*-substituted glycine oligomer, or peptoid

R = side chain      Monomer designation



*Nspe* = (*S*)-*N*-(1-phenylethyl)glycine

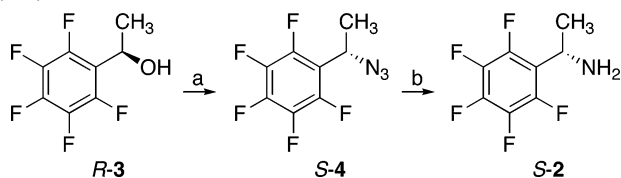


*Nsfe* = (*S*)-*N*-(1-(pentafluorophenyl)ethyl)glycine

peptoid oligomer	monomer sequence (amino to carboxy terminus)	calculated mass	observed mass
<b>5</b>	<i>Nspe</i> –( <i>Nsfe</i> – <i>Nspe</i> ) <sub>2</sub>	1002.4	1003.3 [M + H] <sup>+</sup>
<b>6</b>	<i>Nspe</i> –( <i>Nsfe</i> – <i>Nspe</i> ) <sub>4</sub>	1826.6	1827.6 [M + H] <sup>+</sup>
<b>7</b>	( <i>Nspe</i> ) <sub>5</sub>	822.5	823.5 [M + H] <sup>+</sup>
<b>8</b>	( <i>Nspe</i> ) <sub>9</sub>	1466.8	1467.8 [M + H] <sup>+</sup>
<b>9</b>	( <i>Nsfe</i> ) <sub>5</sub>	1272.2	1273.2 [M + H] <sup>+</sup>
<b>10</b>	( <i>Nspe</i> ) <sub>13</sub>	2111.1	2112.7 [M + H] <sup>+</sup>
<b>11</b>	<i>Nspe</i> – <i>Nsfe</i> –( <i>Nspe</i> ) <sub>2</sub> –( <i>Nsfe</i> ) <sub>2</sub> – <i>Nspe</i> – <i>Nsfe</i> – <i>Nspe</i>	1826.6	1827.4 [M + H] <sup>+</sup>
<b>12</b>	<i>Nsfe</i> –( <i>Nspe</i> ) <sub>8</sub>	1556.7	1579.8 [M + Na] <sup>+</sup>
<b>13</b>	( <i>Nspe</i> )–( <i>Nsfe</i> )–( <i>Nspe</i> ) <sub>7</sub>	1556.7	1557.2 [M + H] <sup>+</sup>
<b>14</b>	( <i>Nspe</i> ) <sub>2</sub> –( <i>Nsfe</i> )–( <i>Nspe</i> ) <sub>6</sub>	1556.7	1557.7 [M + H] <sup>+</sup>
<b>15</b>	( <i>Nspe</i> ) <sub>3</sub> –( <i>Nsfe</i> )–( <i>Nspe</i> ) <sub>5</sub>	1556.7	1557.4 [M + H] <sup>+</sup>
<b>16</b>	( <i>Nspe</i> ) <sub>4</sub> –( <i>Nsfe</i> )–( <i>Nspe</i> ) <sub>4</sub>	1556.7	1557.2 [M + H] <sup>+</sup>
<b>17</b>	( <i>Nspe</i> ) <sub>5</sub> –( <i>Nsfe</i> )–( <i>Nspe</i> ) <sub>3</sub>	1556.7	1579.5 [M + Na] <sup>+</sup>
<b>18</b>	( <i>Nspe</i> ) <sub>6</sub> –( <i>Nsfe</i> )–( <i>Nspe</i> ) <sub>2</sub>	1556.7	1557.8 [M + H] <sup>+</sup>
<b>19</b>	( <i>Nspe</i> ) <sub>7</sub> –( <i>Nsfe</i> )–( <i>Nspe</i> )	1556.7	1557.8 [M + H] <sup>+</sup>
<b>20</b>	( <i>Nspe</i> ) <sub>8</sub> – <i>Nsfe</i>	1556.7	1558.0 [M + H] <sup>+</sup>

<sup>a</sup> All compounds were purified to >97% homogeneity before analysis by CD and NMR. Mass spectrometry data were acquired using either ESI or MALDI-TOF techniques.

**Scheme 1.** Synthesis of (*S*)-1-(Pentafluorophenyl)ethylamine (*S*-2)<sup>a</sup>



<sup>a</sup> Reagents and conditions: (a) 1.1 equiv of diphenylphosphoryl azide (DPPA), 1.1 equiv of diethyl azodicarboxylate (DEAD), 0.9 equiv of PPh<sub>3</sub>, THF, –5 °C, 36 h, 77% yield. (b) 2 equiv of PPh<sub>3</sub>, 9 equiv of H<sub>2</sub>O, THF, 45 °C, 12 h, 63% yield.

number of points (np) was 2048, and 512 points were obtained by linear prediction in the f1 dimension. Square cosine window functions were applied in both dimensions. The spectra were zero-filled to generate f1 × f2 matrices of 4096 × 2048 points.

## Results and Discussion

### Synthesis of (*S*)-1-(Pentafluorophenyl)ethylamine (*S*-2).

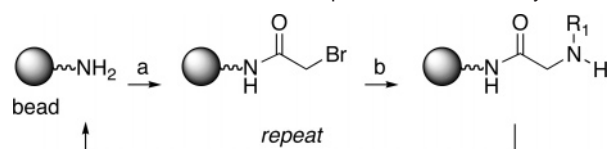
Our two-step synthetic route to (*S*)-1-(pentafluorophenyl)ethylamine (*S*-2) is shown in Scheme 1.<sup>27</sup> In devising a route to amine *S*-2, we sought to overcome a number of potential synthetic difficulties. Foremost of these was the potential for nucleophilic aromatic substitution on the pentafluorophenyl ring; this was indeed observed at elevated temperatures and has proven to be a problematic side reaction in similar systems.<sup>32</sup>

(32) Dilman, A. D.; Belyakov, P. A.; Korlyukov, A. A.; Struchkova, M. I.; Tartakovskiy, V. A. *Org. Lett.* **2005**, *7*, 2913–2915.

We also desired to avoid racemization of the chiral starting material and product. In an attempt to address these issues, we examined a variant of the Mitsunobu reaction using alcohol *R*-3.<sup>33</sup> We found that the initial displacement step did not occur at an appreciable rate at low temperatures (–78 °C), while modest racemization was observed at room temperature. A systematic scan of reaction conditions revealed that the displacement step proceeds with good yield and complete inversion of configuration using 0.9 equiv of triphenylphosphine at 0 °C. Azide *S*-4 was then reacted with triphenylphosphine in the presence of water to afford the desired (*S*)-1-(pentafluorophenyl)ethylamine (*S*-2) in good yield and high enantiopurity (99%). During reaction optimization, we noted the propensities of the azide (*S*-4) and amine (*S*-2) to evaporate when mixed with common organic solvents, possibly due to the formation of azeotropes.<sup>26</sup> This behavior was most pronounced for the azide (*S*-4) and warranted careful distillation for solvent removal. The absolute configuration of *S*-2 was verified by X-ray crystallographic analysis of a crystal of the (+)-2,3-dibenzoyl-*D*-tartrate salt (see Figure S-1, Supporting Information).<sup>34</sup> We found this synthetic route to be reproducible and conductible on a gram scale. Pentafluoroaromatic amine *S*-2 should prove valuable not

(33) Thompson, A. S.; Humphrey, G. R.; Demarco, A. M.; Mathre, D. J.; Grabowski, E. J. *J. Org. Chem.* **1993**, *58*, 5886–5888.

(34) An ORTEP diagram of the *S*-2 salt is shown in the Supporting Information (Figure S-1). X-ray coordinates for *S*-2 have been deposited with the Cambridge Crystallographic Database Centre (CCDC entry no. 281861). These data can be obtained free of charge via [http://www.ccdc.cam.ac.uk/data\\_request/cif](http://www.ccdc.cam.ac.uk/data_request/cif).

**Scheme 2.** Microwave-Assisted Peptoid Submonomer Synthesis<sup>a</sup>

<sup>a</sup> Beads = 200 mesh polystyrene with rink amide linker. Reagents and conditions: (a) 2 M bromoacetic acid, 2 M *N,N*-diisopropylcarbodiimide, DMF, microwave heating (30 s to 35 °C). (b) 1 M amine building block  $\text{NH}_2\text{R}^1$ , DMF, microwave heating (90 s to 95 °C). For details of this synthetic method, see ref 18.

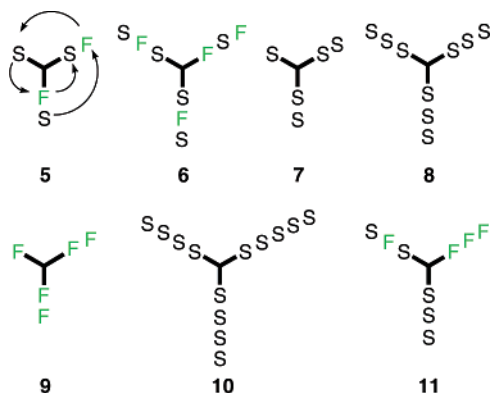


**Figure 2.** Representations of the relative side chain alignments viewed down the putative helical axes of peptoids **5–11**. The N-terminal residue is shown at the bottom of the downward-pointing spoke, with subsequent residues displayed in a counterclockwise, inward-winding spiral, as shown for **5**. S = *Nspe*, green F = *Nsfe*.

only for peptoid synthesis but also as a chiral synthon in a variety of synthetic applications.

**Peptoid Synthesis.** Peptoids are synthesized routinely via the solid-phase submonomer synthesis method developed by Zuckermann et al.<sup>3</sup> This method entails coupling of bromoacetic acid to a solid support, followed by nucleophilic displacement of the bromide with a primary amine to produce peptoid monomer units (Scheme 2). We recently reported a microwave-assisted version of this procedure for the efficient synthesis of peptoids incorporating deactivated benzyl amines and found it to be well suited for the installation of pentafluoroaromatic amine *S-2*.<sup>18,35</sup> This synthetic method was used to generate the subject peptoids of this study (**5–20**, Table 1) in good to excellent crude purities, typically in the range of 70–85%.<sup>28,29</sup> Notably, we did not observe substitution reactions on the fluoroaromatic ring using this protocol. All peptoids were purified to homogeneity (>97%) by preparative RP-HPLC prior to structural analyses. Purities and molar masses of HPLC-purified samples were confirmed by analytical RP-HPLC and mass spectroscopy (Table 1).

**Investigations of  $\pi$ -Stacking in Peptoid Helices.** A series of heteropeptoids and homopeptoids containing (*S*)-*N*-(1-phenylethyl)glycine (*Nspe*) and (*S*)-*N*-(1-(pentafluorophenyl)ethyl)glycine (*Nsfe*) units were synthesized in order to probe  $\pi$ -stacking interactions in peptoid helices (**5–11**, Table 1). The side chain positions viewed down the putative helical axes of these peptoids are shown schematically in Figure 2. Heteropentamer **5** and heterononamer **6** were designed to display alternating aromatic and fluoroaromatic side chains along the

three faces of the peptoid helix. We hypothesized that quadrupolar  $\pi$ -stacking interactions in these heteropeptoids could perturb, and potentially strengthen, helical conformations relative to homooligomer peptoids (**7–10**). We also constructed heterononamer **11** in which an identical number of *Nsfe* units (relative to nonamer **6**) were arranged to maximize the alignment of like monomers along each helical face. This peptoid allowed us to probe for helix disruptions caused by weakened  $\pi$ -stacking interactions. We reasoned that comparison of peptoids with identical monomer compositions, such as **6** and **11**, would most convincingly demonstrate any sequence-dependent phenomena, i.e.,  $\pi$ -stacking, while minimizing interference by other sequence-independent effects, such as local steric interactions. Peptoid homopentamer **7**, homononamer **8**, homo-13-mer **10** (consisting of *Nspe* monomers), and homopentamer **9** (consisting of *Nsfe* monomers) served as important controls for these studies.

The relative helical propensities of peptoids with  $\alpha$ -chiral side chains can be assessed by circular dichroism (CD), a well-established tool for the evaluation of folded structures in peptides and proteins.<sup>36</sup> For peptoids with  $\alpha$ -chiral aromatic side chains, the correlation of relatively intense CD spectra (i.e., diagnostic bands at 192 and 202 nm for the  $\pi$ - $\pi^*$  transition, and at 218 nm for the  $n$ - $\pi^*$  transition) with helical secondary structures has been supported by molecular modeling, NMR, and X-ray crystallography studies.<sup>12</sup> We therefore obtained the CD spectra of peptoids **5–11** to gain further insight into the effect of *Nsfe* units on peptoid secondary structures (shown in Figure 3).

Control *Nspe* homopentamer **7** has been shown previously to display the canonical CD signature for the peptoid helix,<sup>12b</sup> while control *Nspe* homononamer **8** exhibits an atypical, intense CD signature (i.e., a broad, shouldered peak at 203 nm) that corresponds to a nonhelical, “threaded loop” structure.<sup>12c</sup> Reduction in CD intensity at 202 nm has been observed for longer *Nspe* homopeptoids (11–20 units) such as 13-mer **10**, which exhibit enhanced helicity relative to shorter peptoids (5–8 units). Negative CD intensities near 202 nm have been suggested to vary inversely with helical propensity in  $\alpha$ -chiral aromatic peptoids, with deeper minima indicating a higher population of conformations containing *trans*-amide bonds.<sup>12b</sup> As expected, we obtained CD spectra for control homopeptoids **7**, **8**, and **10** that were analogous to those previously reported (Figure 3).

Turning to fluoroaromatic peptoid pentamers **5** and **9**, we found that heteropentamer **5** displayed a CD signature similar in shape to that of the *Nspe* homopentamer control (**7**), yet with a 3-fold weaker intensity at 202 nm (Figure 3, left). The *Nsfe* homopentamer **9** exhibited a further reduction in intensity at 202 nm compared to **5** in its CD signature and an almost complete abolition of the band near 190 nm. These striking effects may be attributable to the fluorination of the aromatic side chains, which could perturb the  $\pi$ - $\pi^*$  transitions of the amide chromophore and produce a blue shift of these bands. Similar blue shifts have been reported in other peptoids with deactivated aromatic side chains.<sup>12a</sup> The disappearance of the 190 nm band may be due to a blue shift below the observable range of these experiments. In contrast, the bands near 215 nm appear to be relatively unaffected by side chain modification, and a comparison of intensities near this wavelength suggests that the helicities of heteropentamer **5** and homopentamers **7** and **9** are similar. Overall, the CD data did not demonstrate

(35) Other researchers have investigated microwave-assisted peptoid synthesis. See: (a) Olivos, H. J.; Alluri, P. G.; Reddy, M. M.; Salony, D.; Kodadek, T. *Org. Lett.* **2002**, *4*, 4057–4059. (b) Fara, M. A.; Diaz-Mochon, J. J.; Bradley, M. *Tetrahedron Lett.* **2006**, *47*, 1011–1014.

(36) Woody, R. W. *Methods Enzymol.* **1995**, *246*, 34–71.

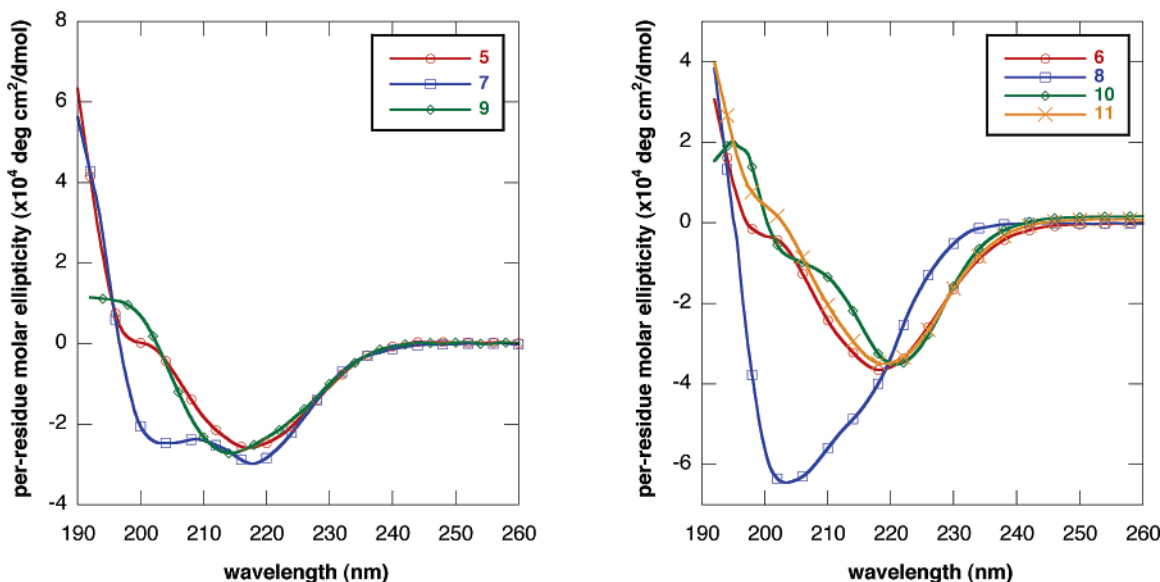


**Figure 3.** CD spectra of peptoids **5**, **7**, and **9** (left) and peptoids **6**, **8**, **10**, and **11** (right) at  $60 \mu\text{M}$  in acetonitrile. Spectra were collected at  $25^\circ\text{C}$ .

that quadrupole-enhanced, intramolecular  $\pi$ -stacking is operative in these systems.

We next examined the impact of *N*sfe units on the structures of longer peptoid systems, i.e., nonamers **6**, **8**, and **11** (Figure 3, right). As peptoid nonamers composed largely of  $\alpha$ -chiral, aromatic monomers had been shown to significantly populate alternative, nonhelical conformational states (*vide supra*),<sup>12b</sup> these systems provided latitude for enhancement of helical structure. We were gratified to observe that the CD signature of the alternating heteronamer **6** indicated a dramatic increase in helical propensity relative to the *N*spe homonamer **8** and corresponded closely to that of the longer, helical *N*spe 13-mer **10**.<sup>12b</sup> However, heteronamer **11** exhibited a nearly identical CD signature to peptoid **6**, despite the altered arrangement of aromatic quadrupoles along the faces of this peptoid. These results suggested that intramolecular  $\pi$ -stacking is not the dominant factor in the stabilization of canonical helices for this peptoid class.

We also considered the possibility that intermolecular interdigitation of peptoid side chains mediated by aromatic interactions could stabilize peptoid helices. Although prior work by Wu et al. has demonstrated that the structure of an *N*rpe hexamer is independent of concentration between  $0.8$  and  $64 \mu\text{M}$  in acetonitrile,<sup>12b</sup> we reasoned that the distinctive quadrupole and/or solubility characteristics of *N*sfe monomers could facilitate stabilization by this mechanism. Solutions of *N*spe homopentamer **7** and *N*sfe homopentamer **9** (each  $60 \mu\text{M}$ ) were mixed, and the CD spectrum of the mixture was recorded (Figure 4). This trace was simply the average of the spectra of its constituents, as would be expected if no aggregation-induced folding was to occur. The peptoid mixture then was heated to  $65^\circ\text{C}$  and subsequently left standing at room temperature in an attempt to overcome potential kinetic barriers to interdigitation by annealing; however, the CD spectrum of the mixture remained unchanged. The mixture was finally diluted with an equal volume of water to determine if increased solvent polarity might induce interdigitation by hydrophobic aggregation, but only a small increase (within the error range determined for dilution by volume) in helicity was observed. We note that any increase in helicity could also arise from the enhanced hydro-

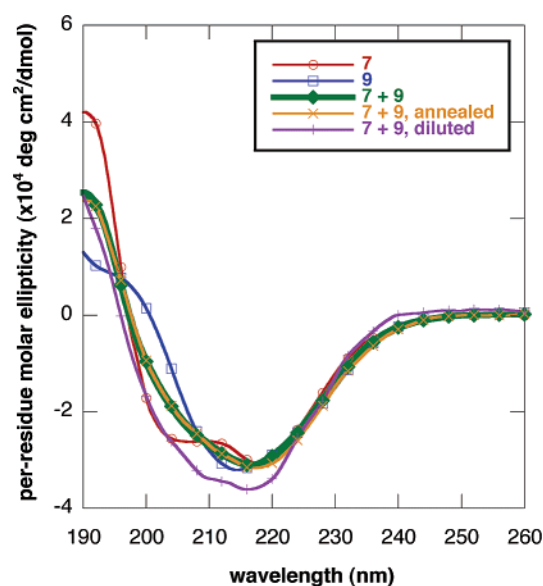


**Figure 4.** CD spectra of  $60 \mu\text{M}$  solutions of peptoids **7** and **9** in acetonitrile (red and blue), a 1:1 mixture of **7** and **9** (total peptoid concentration was  $60 \mu\text{M}$  in acetonitrile) before (green) and after (orange) attempted annealing, and a 1:1 mixture of **7** and **9** (total peptoid concentration of  $30 \mu\text{M}$ ) in 1:1 acetonitrile/water (purple). Spectra were collected at  $25^\circ\text{C}$ .

phobic collapse of unassociated, individual peptoids, as has been previously suggested.<sup>37</sup> Overall, these experiments did not provide compelling evidence that intermolecular interdigitation of the peptoid side chains stabilizes helical structure under these conditions. Studies examining this phenomenon over a wider range of conditions are ongoing in our laboratory, however, in order to further assess the possibility of aggregation-induced folding in these systems.

The studies above suggest that intramolecular, quadrupole-enhanced  $\pi$ -stacking may not play an appreciable role in stabilizing peptoid helices. The CD spectra of heteronamer peptoids **6** and **11** containing identical numbers of *N*sfe monomers were the most notable in this regard; these were

(37) Bradley, E. K.; Kerr, J. M.; Richter, L. S.; Figliozzi, G. M.; Goff, D. A.; Zuckermann, R. N.; Spellmeyer, D. C.; Blaney, J. M. *Mol. Diversity* **1997**, *3*, 1–15.

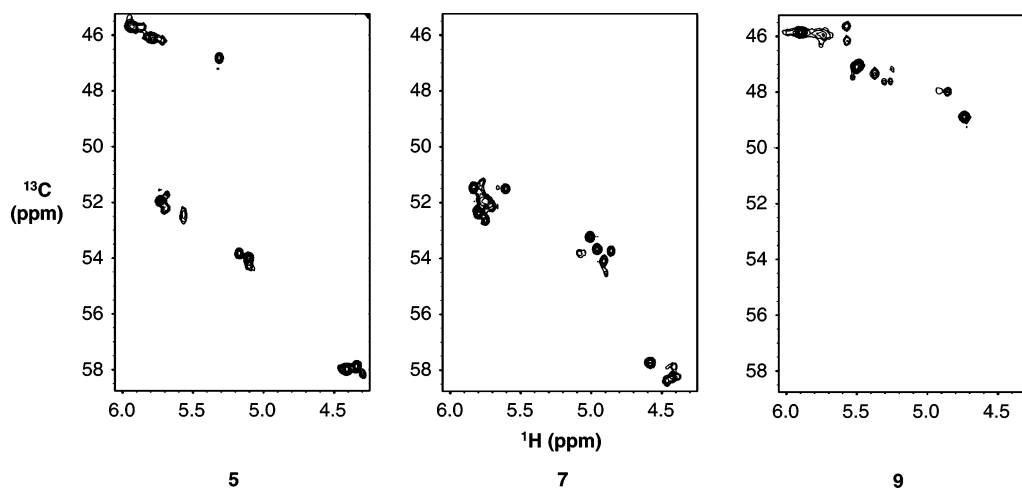


**Figure 5.** Methyne regions in the HSQC NMR spectra of the peptoid pentamers **5**, **7**, and **9**. Samples were prepared in acetonitrile- $d_3$  (ca. 6 mM) and analyzed at room temperature (24 °C). For full HSQC spectra, see Supporting Information (Figures S-2 to S-4).

nearly equal in intensity, regardless of the sequence of aromatic and pentafluoroaromatic groups along the helical faces. These data caused us to speculate that periodic incorporation of  $\alpha$ -chiral aromatic side chains in peptoids may stabilize helices by other means, such as hydrophobic or cooperative steric effects. However, we could not completely rule out the possibility that intra- or intermolecular  $\pi$ -stacking may still be operative but is not directly observable in these experiments. We therefore obtained heteronuclear single quantum coherence (HSQC) NMR data for pentamer peptoids **5**, **7**, and **9** (Figure 5) in an effort to obtain additional information about the behavior of these systems. Analysis of the peptoid side chain methyne correlations in this type of NMR experiment has been used previously to assess the conformational distribution of peptoids in solution.<sup>12d</sup> As the peptoid helix consists exclusively of *cis*-amide bonds, the relative integrations of *cis*- and *trans*-amide correlations have been used as secondary indicators of peptoid helicity. Furthermore, the number of distinct methyne correlations has also been used to qualitatively evaluate conformational homogeneity. We expected that the introduction of strongly electron-withdrawing groups such as amine **S-2** would decrease the barrier for *cis*–*trans* isomerization of the tertiary amides,<sup>38</sup> resulting in increased backbone flexibility. We thus analyzed samples in acetonitrile- $d_3$  at 24 °C with peptoid concentrations of ca. 6 mM.

A comparison of the HSQC NMR spectra revealed a reduced number of correlations for *Nsfe* homopentamer **9** relative to pentamers **5** and **7** (Figure 5), initially implying greater conformational homogeneity in this system relative to the other pentamers. However, the broader line widths in the *Nsfe* homopentamer **9** spectrum suggested that this peptoid could be subject to dynamic conformational interconversion on the NMR experimental time scale at room temperature. This interconversion of peptoid conformers has previously been observed in similar peptoid systems, albeit at rates that presumably did not complicate the assessment of conformational distributions.<sup>20</sup> Alternatively, line broadening might also be caused by aggregation; however, data acquisition at concentrations approaching the detection limit of the NMR spectrometer (below 1 mM) did not improve spectral quality (data not shown). Regardless

of the cause, this signal broadening complicated the rigorous quantification and integration of the methyne correlations for **9**, although a semi-quantitative analysis of the pentamer spectra revealed that the overall percentages of *cis*- and *trans*-amide bonds were similar (see Table S-1, Supporting Information). Notably, the *Nsfe* residues of **5** (at positions 2 and 4) exhibited a significantly higher *cis*:*trans*-amide ratio than the *Nspe* residues (approximately 3:1 versus 1:1). As “fraying” of the peptoid helix at the C-terminus has been observed previously,<sup>20</sup> this finding could be attributed to a higher degree of helicity at internal positions within the oligomer, as opposed to the termini, and suggests that peptoid **5** is indeed structured.

We also obtained rotating frame Overhauser spectroscopy (ROESY) NMR of spectra of all three homopentamers (see Figures S-5 to S-7, Supporting Information) in order to reinforce the structural parity of this peptoid series. These spectra exhibited similar contact patterns that suggest the spatial relationships between protons are comparable among the members of this peptoid class. Overall, the congruity of these ROESY and HSQC NMR spectra, in conjunction with the well-defined CD spectra exhibited by the pentamers, implies that these systems are structurally similar. Ongoing studies in our laboratory are directed at further characterizing the solution-phase behavior of several of the peptoid systems introduced herein by NMR. This work is expanding our understanding of the folding of perfluoroaromatic peptoids and will be reported in due course.

**Influence of Pentafluoroaromatic Monomers on Peptoid Nonamer Structure.** We were intrigued by the dramatic enforcement of helicity observed in the CD spectra of peptoid nonamers upon *Nsfe* incorporation, e.g., peptoids **6** and **11**. However, the experiments outlined above suggested that intramolecular  $\pi$ -stacking interactions between side chains were not primarily responsible for this effect. During the course of these investigations, Huang et al. reported an NMR structure of the *Nspe* homonamer **8** that resembled a “threaded loop” (shown in Figure 6, left).<sup>12e</sup> This structure is stabilized by intramolecular hydrogen bonds between the peptoid termini and several backbone amide carbonyls (residues 5, 7, and 9 in Figure 6, left). The structural necessity of these contacts was demonstrated by several studies in which the structure was disordered upon titration with protic solvents. We hypothesized

(38) Eberhardt, E. S.; Panisik, N., Jr.; Raines, R. T. *J. Am. Chem. Soc.* **1996**, *118*, 12261–12266.

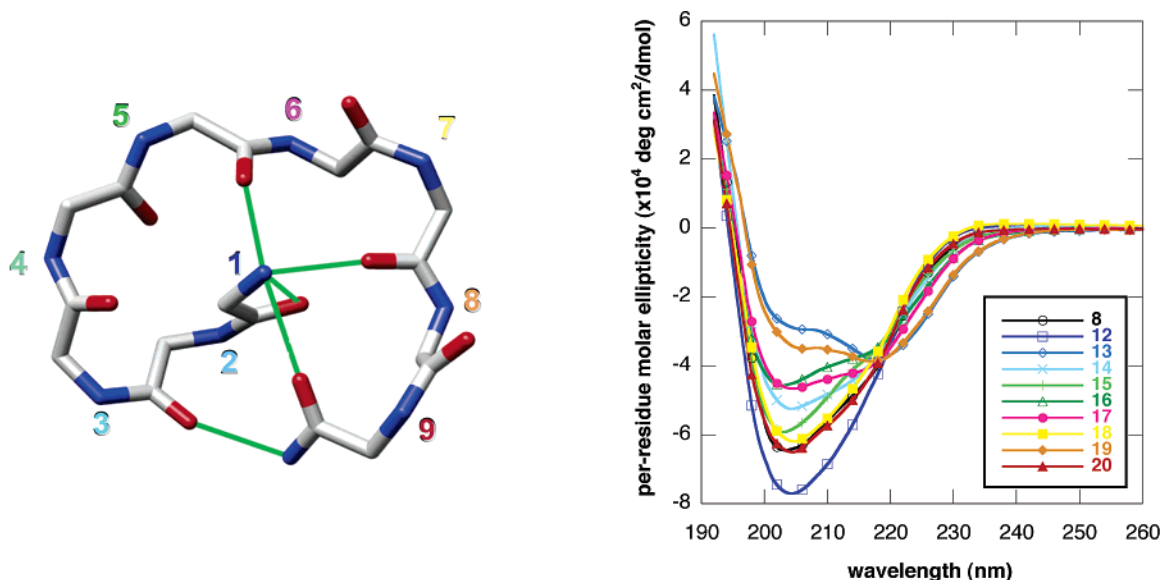


**Figure 6.** (Left) Representative NMR structure of the Nspe nonamer **8** in acetonitrile.<sup>40</sup> Numbers indicate relative positions of amide side chains on the peptoid backbone (from amino to carboxy terminus). Backbone atoms are shown only; red = oxygen; blue = nitrogen; gray = carbon. Putative hydrogen bonds are shown as green lines. (Right) CD spectra of peptoids **8** and **12–20** at 60  $\mu$ M concentrations in acetonitrile. Trace colors correlate with those of the Nsfe position numbers in structure at left. Spectra were collected at 25  $^{\circ}$ C.

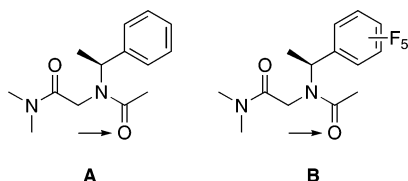
that Nsfe pentafluoroaromatic rings could significantly deactivate the proximal backbone amides as hydrogen bond acceptors,<sup>39</sup> disrupting the threaded loop structure and enhancing the helicity of peptoids such as **6** and **11**. This behavior could be exploited to selectively “tune” the hydrogen bonding capacities of each backbone carbonyl, providing an approach for rationally controlling peptoid structure while simultaneously retaining the established steric profile for peptoid helix formation. We tested this hypothesis by performing an Nsfe “scan” of the Nspe nonamer **8**, in which a series of nine peptoids were synthesized, each incorporating the Nsfe monomer at a different location (**12–20**, Table 1). The CD spectra of these peptoids were obtained and analyzed to assess the structural impact of the pentafluoroaromatic side chain at each location (Figure 6, right).

The position of the single Nsfe monomer in the nonamer peptoid clearly had remarkable consequences for the folding of this peptoid class. The intensities of the CD bands near 192, 202, and 218 nm have been used previously to qualitatively assess the relative populations of helical and looped secondary structures adopted by Nspe homonamer **8**. As described above, the threaded loop structure is characterized by a strong minimum near 205 nm in its CD spectrum, whereas the helical

conformation is diagnosed by the appearance of several minima, including an intense minimum at 218 nm.<sup>12e</sup> We analyzed the CD spectra of peptoids **12–20** according to these criteria (Figure 6, right). As we predicted, the incorporation of fluoroaromatic side chains near critical hydrogen bonding positions significantly disrupted the threaded loop structure (positions 3, 6, and 8; **14**, **17**, and **19**). We also discovered that the threaded loop is disrupted by incorporation of fluoroaromatic side chains at two amides not previously implicated in hydrogen bonding (positions 2 and 5; **13** and **16**); this disruption is nearly absolute in the former case. An examination of the three-dimensional structure of the threaded loop did not reveal any significant steric repulsion that might result from the increased size of the Nsfe monomer relative to Nspe; however, the carbonyl of residue 1 is located four bonds from the N-terminal ammonium protons and is ideally situated to form an intramolecular hydrogen bond to the amine terminus. Our data suggest that the formation of such a hydrogen bond may play a pivotal role in the formation and/or stabilization of the loop structure. The cause of the disruption resulting from installation of the fluoroaromatic side chain at residue 5 is unclear, but we speculate that formation of a hydrogen bond to this amide may also play a role during folding. In contrast, fluoroaromatic side chains at positions 4, 7, and 9 (**15**, **18**, and **20**) produced inconsequential changes in the CD spectra of these peptoids relative to homonamer **8**.<sup>41</sup>

Most strikingly, we found that installation of the Nsfe monomer at the amino terminus (in peptoid **12**) significantly *stabilized* the threaded loop structure relative to the helical structure. We reasoned that inductive withdrawal of electron density at this terminus by the pendant fluoroaromatic group likely increases both the acidity and positive charge of the ammonium group, with concomitant strengthening of its hydrogen bonding potential. We titrated an acetonitrile solution

(39) Preliminary calculations at the RHF 6-31G\* level show ca. 1.5 times more electron density at the carbonyl oxygen of an Nspe peptoid monomer system (**A**) relative to that of an analogous Nsfe monomer system (**B**) (see structures below; carbonyls of interest indicated). The electron density ratio was determined by comparing both the electrostatic potential and HOMO maps of **A** and **B**. The calculations were performed using Spartan '04 for Macintosh (Wavefunction, Inc., Irvine, CA; Kong et al. *J. Comput. Chem.* **2000**, *21*, 1532–1548; see Supporting Information for full author list). Ongoing studies in our laboratory are focused on further examining the electrostatics and conformational preferences of these and other monomeric peptoid systems at higher levels of theory.



(40) The atomic coordinates for this NMR structure were graciously provided by the authors in ref 12e.

(41) We note that excessive withdrawal of electron density from the backbone amides would likely increase their susceptibility to hydrolysis and nucleophilic attack (e.g., imides); however, we did not observe any degradation of Nsfe-amide bonds during the synthetic work and structural analyses described herein.



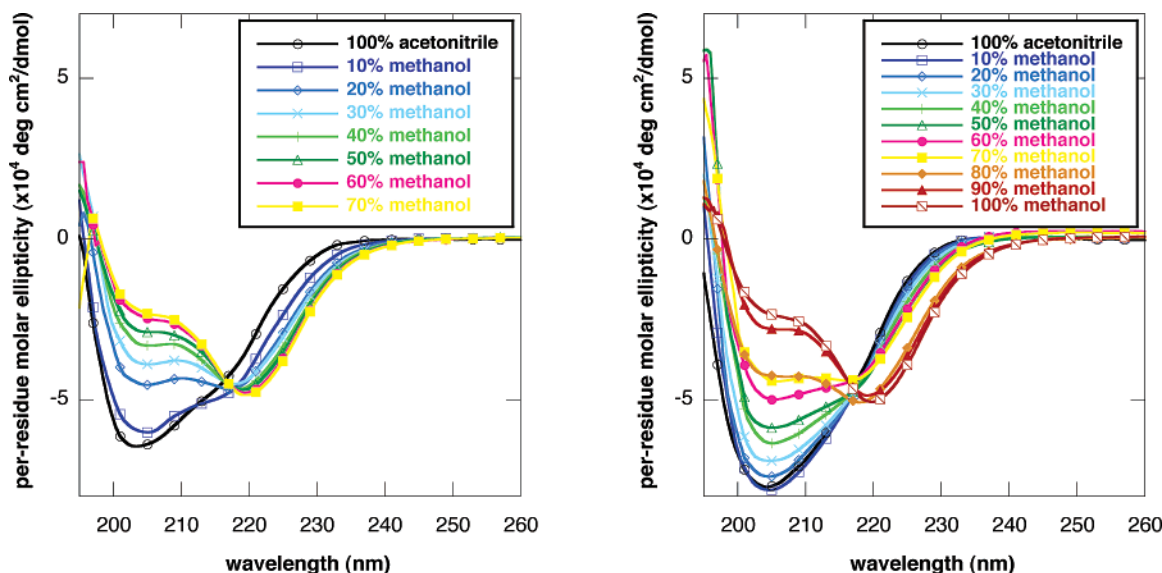


**Figure 7.** CD spectra of homonomers ( $Nspe$ )<sub>9</sub> (**8**) (left) and  $Nsfe$ -( $Nspe$ )<sub>8</sub> (**12**) (right) at 60  $\mu$ M concentrations in acetonitrile/methanol solutions. Spectra were collected at 25 °C.

of **12** with the polar protic solvent methanol, analyzed these solutions by CD to assess the resistance of **12** to denaturation, and compared these data to those obtained using the  $Nspe$  homonomer **8**. As previously reported, the threaded loop structure formed by **8** was completely lost upon titration to approximately 50% methanol (Figure 7, left).<sup>12c</sup> In contrast, the loop structure formed by heteropeptoid **12** was extremely resistant to titration with methanol, withstanding total denaturation until the titration was complete (Figure 7, right).

These findings demonstrate that peptoid nonamer structure can be controlled by the strategic incorporation of  $Nsfe$  monomers. Our data suggest that these monomers serve to control folding by modulating the hydrogen bonding potentials of proximal amides.<sup>39</sup> This hypothesis is supported by our previous observation that the nucleophilicity, and presumably also the electron density, of deactivated benzyl amines are significantly reduced relative to those of nonsubstituted benzyl amines.<sup>18</sup> The stronger helical CD signatures displayed by peptoids **6** and **11** (with  $Nsfe$  monomers at positions 2, 4, 6, and 8, and 2, 4, 5, and 8, respectively), as well as other related systems previously examined in our laboratory,<sup>18</sup> can be explained according to this rationale. Furthermore, incorporation of this pentafluoroaromatic side chain at the amino terminus dramatically enhances the capabilities of the latter as a hydrogen bond donor, stabilizing the unique threaded loop structure while simultaneously preserving the well-established steric profile known to promote peptoid folding. Notably, this is accomplished without introducing other heteroatoms such as oxygen or nitrogen that could potentially compete for hydrogen bonds and prevent proper folding. The stabilized,  $Nsfe$  threaded loop structure largely persists in the presence of protic solvents, which more closely mimic the aqueous media relevant to biological function. As such, this research represents an initial step toward the construction of new, water-stable peptoid architectures that could be explored within this context.

## Conclusions

We have discovered a new design principle for peptoid folding based on the incorporation of pentafluoroaromatic side

chains. This work was enabled by the development of an efficient synthesis of (*S*)-1-(pentafluorophenyl)ethylamine (*S*-**2**), which we found to be highly compatible as a building block for peptoid construction. Systematic CD and NMR studies did not suggest that incorporation of amine *S*-**2** into peptoids stabilizes helical structure by enhancing  $\pi$ -stacking interactions along the helical face. Rather, we have discovered that the judicious incorporation of this amine can effectively control the folding of peptoids by modulating the hydrogen bonding capacities of nearby heteroatoms. Moreover, the distinctive threaded loop structure can be effectively promoted, even in predominantly protic solvents, using this new pentafluoroaromatic peptoid building block.

We contend that the strategic incorporation of fluoroaromatic and perhaps other electron-deficient aromatic side chains<sup>18</sup> into peptoids is a straightforward and effective strategy for controlling peptoid structure via hydrogen bonding interactions. This design principle should significantly expand the scope of peptoid design and enhance the utility of peptoids for a broad range of applications. In the future, we envisage the co-introduction of hydrogen bonding and fluoroaromatic peptoid side chains, which could dramatically broaden this strategy by increasing the number of tunable hydrogen bonds. These additional tunable interactions could provide access to a diverse range of new peptoid secondary structures, potentially with increased aqueous solubility. Indeed, peptoids represent a unique foldamer class with which to explore this tactic, as their distinguishing tertiary amide backbones (as opposed to the secondary amide backbones of typical  $\alpha$ - and  $\beta$ -peptides) would not compete with hydrogen bond donor groups installed on side chains. We also anticipate that this hydrophobic side chain could facilitate the hydrophobic collapse of water-soluble peptoids to generate tertiary structures, as has been recently demonstrated.<sup>42</sup> Ongoing work in our laboratory is directed at further developing these design tactics in an effort to expand the existing repertoire of peptoid folding motifs beyond the established helix and threaded loop structures.

(42) Lee, B.-C.; Zuckermann, R. N.; Dill, K. A. *J. Am. Chem. Soc.* **2005**, *127*, 10999–11009.

**Acknowledgment.** We thank the NSF (CHE-0449959), Research Corporation, the Greater Milwaukee Foundation Shaw Scientist Program, CEM Corporation, and the UW-Madison for financial support of this work, and the W. M. Keck Foundation for support of instrumentation at the UW Keck Center for Chemical Genomics. Support of the NMR facilities at UW-Madison by the NIH (1 S10 RR13866-01, 1 S10 RR04981-01, and 1 S10 RR0 8389-01) and the NSF (CHE-0342998, CHE-9629688, CHE-8813550, and CHE-9208463) is gratefully acknowledged. We thank Professors Annelise Barron and Ishwar Radhakrishnan for providing the structural coordinates for the peptoid threaded loop, Dr. Charles Fry and Dr. Monika Ivancic for assistance with NMR spectroscopy, Dr. Ilia Guzei for X-ray

crystallographic analyses, Professor Thomas Brunold for use of his CD instrumentation, Grant Geske for modeling studies, and Professors Annelise Barron, Kent Kirshenbaum, and Samuel Gellman for numerous helpful discussions.

**Supporting Information Available:** General experimental information, details of microwave instrumentation, X-ray crystal structure analysis of *S*-2/(+)-2,3-dibenzoyl-*D*-tartrate salt complex, NMR spectra of a peptoid pentamers **5**, **7**, and **9**, and complete ref 39. This material is available free of charge via the Internet at <http://pubs.acs.org>.

JA065248O